GAMMA RAY SHIELDING PROPERTIES OF MORTARS CONTAINING SLAG

by

James Richard Dughi

A Thesis Submitted to the
Graduate Faculty in Partial Fulfillment of
The Requirements for the Degree of
MASTER OF SCIENCE

Major Subject: Engineering

Approved:

Iowa State College
1957

TABLE OF CONTENTS

I. INTRODUCTION

Increased use of radioactive materials and the interest in nuclear power reactors has added impetus to the search for good shielding materials. Some of the desirable properties for a nuclear reactor shield are (1) high density to minimize thickness, (2) high content of light elements for the degradation of the neutron flux, (3) high content of heavy elements for the degradation of gamma rays, (4) low cost, (5) ease of fabrication and installation, (6) reasonable structural strength, stability under irradiation and stability under hot, moist or dry conditions.

Water and the hydrocarbons are effective neutron shields but are inefficient gamma ray shields. Lead is an excellent gamma ray shield but is a poor neutron shield. It would be necessary to combine water and lead to obtain an efficient reactor shield. Concrete is one of the few materials that combines all the above desirable qualities to any satisfactory degree. For this reason concrete has been used rather extensively as a shielding material.

Gallaher and Kitses (1) state that the required concrete thickness is determined by the required gamma ray attenuation, and not by the required neutron attenuation. The light element content of the concrete is usually sufficient to reduce the neutron flux to the desired level when the gamma rays have been reduced to the desired level.

The theory of gamma ray attenuation has been well established and discussions of this theory can be found in any standard nuclear physics text book such as Kaplan (2, pp. 322-356).

The basic property of the attenuation of gamma rays is the exponential decrease in the intensity of radiation as a homogenous beam passes through a thin slab of material. For a homogenous beam of initial intensity I_0, with intensity I after passage through a material of thickness x, the relationship is

$$I = I_0 e^{-\mu x}$$

where the constant μ is defined as the linear absorption coefficient. This constant can be determined by either theoretical or experimental means.

The interaction of gamma rays with matter is described by three major processes, namely, (1) photoelectric absorption, (2) Compton scattering, and (3) pair production. The absorption coefficient depends on the nature of the absorbing material as well as the energy of the incident photon, and no single formula or range-energy curve has been obtained for all materials. For the probability of each of the above three processes as a function of energy, formulas can be derived by the use of quantum mechanics. The probability can be expressed as an absorption coefficient or cross section. The total absorption coefficient is the sum of the three partial cross sections evaluated as a function of energy for a given material.

The contribution of each process varies with the energy and the material. In the photoelectric effect all the energy of the photon is transferred to a bound electron which is ejected from the atom. This effect is most important for gamma rays with energies less than 0.5 Mev. and for absorbers of high atomic number.

In Compton scattering the incident photon is scattered by an atomic electron. The photon moves off at an angle with its initial direction and

with less than its initial energy. This effect is most important for absorbers of low atomic number and is the predominant process even in elements of high atomic number when the energy range of the incident photon is between 0.6 Mev. and 3 Mev.

The pair production process involves the creation of a positron-electron pair by the absorption of a photon. The process cannot take place unless the photon energy is at least 1.02 Mev. This process is important for high gamma ray energies and for elements of high atomic number.

The theoretical results for the evaluation of absorption coefficients have been collected and compared with experimental results in a review article by Davisson and Evans (3). The results indicate excellent agreement between theory and experiment.

To obtain valid experimental results the restrictions of the equation describing gamma ray attenuation must be considered. First, the incident beam was considered to be mono-energetic. Second, the beam was considered to be collimated, i.e., scattered radiation left the beam and was not rescattered back into the beam. Third, the absorber was thin. Experimental arrangements which meet these restrictions are considered to have "good geometry". For "good geometry" arrangements, the gamma ray attenuation equation is valid, and the absorption coefficient can be determined by measuring beam intensities for various absorber thicknesses.

II. REVIEW OF LITERATURE

The thickness of a concrete shield is determined by the required reduction in gamma ray intensity. Snyder (4, p. 123) states that as a rough approximation, the ratio of the density of two materials is equal to the ratio of their absorption coefficients in the energy range of 1 Mev. to 3 Mev. Thus, high density concretes are desirable in order to decrease the required thickness of the shield.

Heavy concretes have been used as the shielding material for many of the reactors now in operation. The review article by Gallaher and Kitzes (1) lists the composition and mixing formula for several of these heavy concretes. It also compares the properties for the various concretes. Composition and shielding properties for most of the heavy concretes in use, or proposed, have been collected and reviewed by Snyder (4) and Hungerford (5, pp. 715-732). In most cases, the density of the concrete is increased by using iron filings or punchings as the heavy aggregate. The concrete density can be doubled by this method. By using a barytes ore as both the fine and course aggregate, the density of the concrete can be increased 50 percent.

The selection and placing of high density concretes is discussed by Davis (6). The special techniques required to obtain a sound shield are discussed as well as the difficulties encountered with embedded items and access holes through the shield.

A cost comparison of high density concrete shields is made by Lane (7). Since special techniques and handling equipment are required for

high density concretes the cost is considerably higher. The gain in shielding volume reduction for high density concretes must be balanced against the increased cost. The space available for shielding must also be considered when determining the shielding material.

III. INVESTIGATION

The use of slag as a fine aggregate in mortar was studied to determine the effect of the slag on the absorption coefficient. Since a mortar of this type can be mixed and cast by standard techniques, the cost as compared to standard mortar will be directly proportional to the cost of the slag as compared to the cost of the sand normally used in a given area. Since power reactors will probably be situated near industrial areas, the cost of slag will probably compare favorably with the cost of the sand.

Heavy mortar could be used with the presently used high density course aggregates thereby further increasing the density of the concrete with little or no cost increase.

A study was made to determine whether there would be any gain in the gamma ray attenuation by keeping the mortar saturated with water.

The study was conducted at only one energy level, 1.25 Mev.

IV. EQUIPMENT AND MATERIAL

A. Radiation Source

A Co^{60} source of approximately 2.5 millicuries strength was used in this study. The source was present as cobalt chloride in an aluminum container. The source was cylindrical in shape with a diameter of 1/8 inch and 1/16 inch thick. The aluminum container was also a cylindrical disk with a 3/8 inch diameter and 3/16 inch thick. The source was contained in a 4 by 4 by 6 inch lead block. A 7/8 inch hole was drilled in one of the 4 by 6 inch faces to a depth of 2-1/4 inch. The source was placed in the bottom of this hole with the axis of the cylinder parallel to the axis of the hole.

The Co^{60} source has two photons emitted in cascade with energies of 1.17 Mev. and 1.33 Mev. For this study an average energy of 1.25 Mev. was used and no corrections were made for self absorption or absorption in the aluminum container. The source has a half life of 5.2 years so no correction was necessary for its gamma ray decay.

B. Detector and Apparatus

The detector used was a mica end window Geiger-Mueller tube, model D33, manufactured by the Nuclear Instrument and Chemical Corporation. The mica end window was 3.5 mg/cm^2 thick. The diameter of the tube measured 1.375 inches at the window. The tube was operated at a 950 volt potential.

The scaler used was a model 200 scaler manufactured by the Radiation

Instrument Development Laboratory. The scaler was operated with the discriminator set at 60 and with the gain set as 1/16. It was found that with the gain set any higher, the sensitivity of the instrument was so great that it was effected by outside disturbances.

Tests were conducted with the apparatus on a 100- microcurie Co^{60} source. The results showed the setup to be 2 percent efficient for the detection of gamma rays.

C. Shielding

Several 2 by 4 by 8 inch lead bricks were built up around the source and the detector tube. The bricks were so placed as to provide 4 inches of lead around both the source and the detector tube to reduce the scattering effect. The four inches of lead around the source and detector reduced the intensity of the incident beam to less than 0.01 percent of its initial intensity.

Four lead blocks, labeled B, C, D, and E, and whose dimensions are shown on Figure 1, were used to collimate the radiation beam. The blocks were also present to reduce the radiation scattered by the absorbers from reaching the detector.

D. Geometry

A photograph showing the general experimental layout is shown in Figure 2. The dimensions for the layout are given in Figure 1. This is similar to the configuration used by Davisson and Evans, (8) for the determination of absorption coefficients.

The holes in the collimating blocks are of such a size as to give the

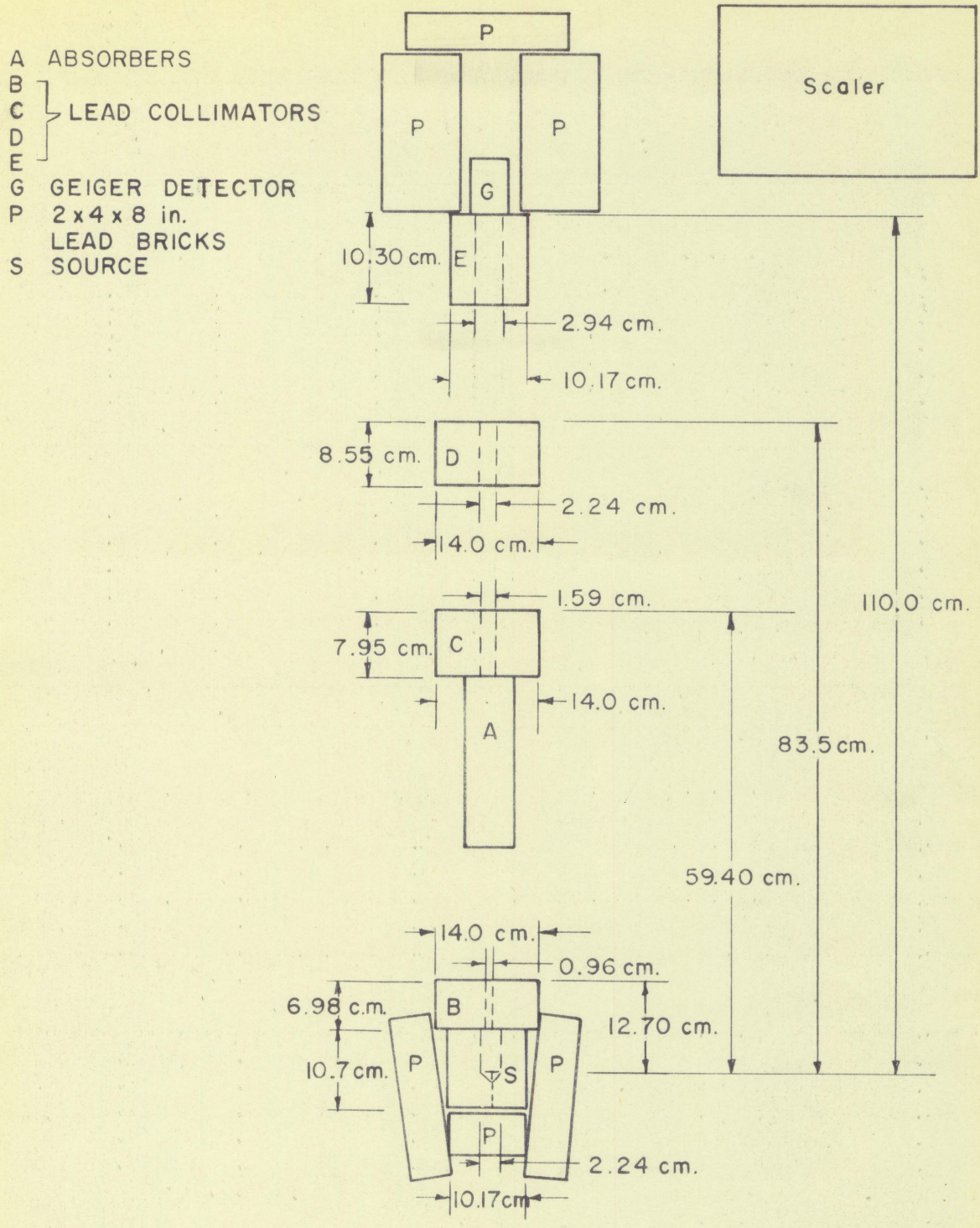

Figure 1. Experimental setup showing dimensions.

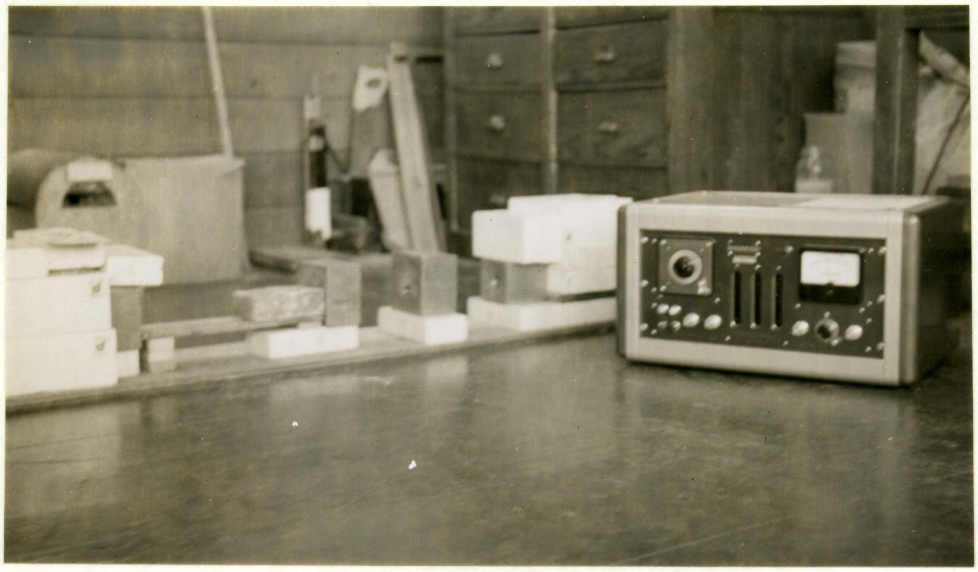

Figure 2. Experimental layout.

detector tube an unrestricted view of the source. These blocks eliminate much of the scattered radiation since their thickness reduces the intensity of a beam normal to their face to 0.5 percent of the initial intensity.

Since the average source energy was 1.25 Mev., the attenuation of the photons was due almost entirely to Compton scattering. The analysis of multiple scatterings is complicated, and the results are involved. The analysis for single scattered photons has been presented by Davisson and Evans (3). The results are an extension of the work originally done by Heitler (9).

For the case where the absorber is not close to either the source or the counter, the ratio of singly scattered photons striking the detector

to the number of unscattered photons striking the detector, S/B is expressed as

$$S/B = N_e \times {}_e\sigma_s^{\theta_o} .$$

where N_e is the number of electrons per cubic centimeter of absorber, X is the absorber thickness, and ${}_e\sigma_s^{\theta_o}$ is the cross section for the total photon energy scattered through an angle θ_o. For small angles, θ_o less than 5.

$${}_e\sigma_s = \pi \frac{e^2}{m_o c^2} \theta_o^2 .$$

For the experimental layout as shown in Figure 1 the maximum scattering angle was determined to be 3.2°. The angle was measured in the following manner. A line was drawn from one edge of the source across the center line to the edge of the hole in collimating block C at the absorber face. A line from this point was drawn across the center line to the edge of the detector face visible behind collimating block D. The angle between these two lines was defined as the maximum single scattering angle.

Ten cm. of lead were assumed as the extreme case for this study, S/B was computed to be .0208. Approximately 2 percent of the total count would be the maximum possible error caused by singly scattered photons reaching the detector. No corrections were made to the counting data for this scattering.

In view of the result, any variation in the detector efficiency as a function of energy of the incident photon can be ignored.

In order to determine the accuracy of the experimental setup, an absorption curve for lead was determined and is shown in Figure 3. Standard

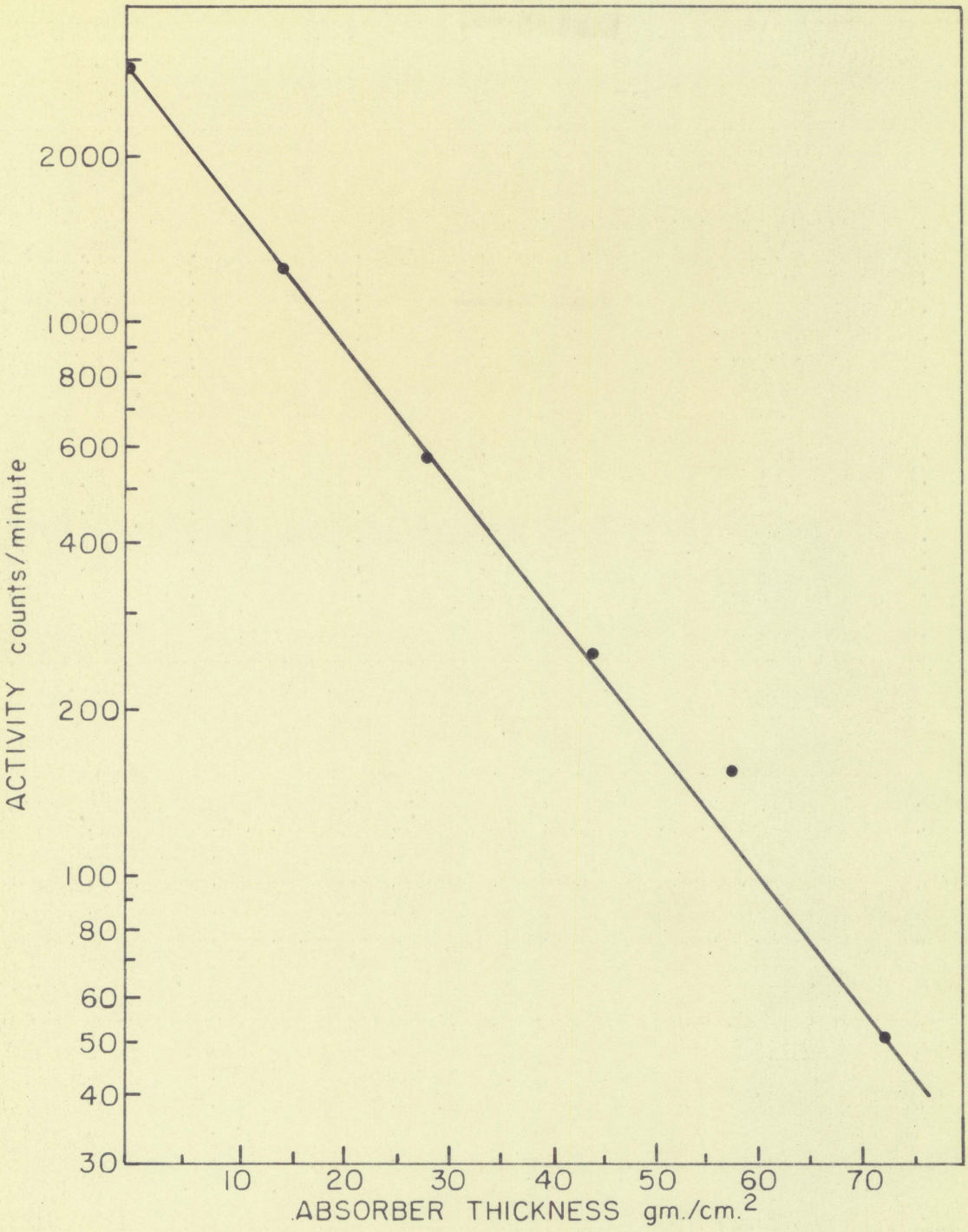

Figure 3. Lead absorption curve.

deviation for the counting was maintained below 2 percent. The value of the mass absorption coefficient was determined to be .0570 cm^2/gm. Davisson and Evans (3) list the mass absorption coefficient for lead as .057h for 1.25 Mev.

This absorption curve indicates that while multiple scattering and secondary radiation due to annihilation radiation or bremsstrahlung were ignored the effects are negligable.

E. Absorbers

The absorbers used were 2 by 2 by 4 inch mortar blocks. The composition of the blocks was varied, and the absorption coefficient was determined for each composition. The composition and fabrication of each set of blocks is discussed in detail in the section on Procedures. The chemical analysis of the ingredients was not obtainable but Table 1 shows the normal compositions of the cement and slag. The sand was assumed to be 100 percent SiO_2, and no information was available concerning the fly ash.

Table 2 shows the particle distribution as determined by screening tests and Table 3 gives the densities of all the ingredients. The data given in Table 2 are also plotted in Figure 16.

Table 1. Chemical composition of cement and slag in percent weight

	SiO_2	Fe_2O_3	Al_2O_3	CaO	MgO
Portland cement Type I[a]	23	4	8	63	2
Slag[b]	40	30	20	8	2

[a]Values are average values as reported in Ref. 5, p. 723.

[b]These are average values as reported by the producer.

Table 2. Particle size of sand and slag

Screen size	Percent passed screen	
	Sand	Slag
1.49 in.		100
.742 in.		97
.371 in.	100	94
No. 4	98	89
No. 8	88	68
No. 16	64	32
No. 50	8	3
No. 100	2	1

Table 3. Densities of materials

Material	Sand	Slag	Fly ash	Portland cement Type I
Density, gm/cm^3	2.55	2.80	2.75	3.20

V. PROCEDURES

As noted previously the composition of the mortar blocks was varied for this investigation. In all, eight different mixtures were tested. The compositions of the eight mixtures are shown in Table 4 and are labeled A through H. In mixtures A to G the percentage by weight of cement and water were held constant. For mixtures A to E, the amount of slag replacing the sand was varied. As the slag content was increased, the mixtures appeared to become very harsh. As an aid to reducing the courseness, fly ash was added as part of the fine aggregate in mixtures F and G. In mixture H an attempt was made to increase the total aggregate using slag and fly ash.

The procedures used for mixing and casting of the blocks were the same for all mixtures. The cement, fly ash if present, and about one-fourth of the aggregate were thoroughly mixed. The water was added and again mixed with a hand trowel. The remainder of the aggregate was added in small amounts and mixed. When all the aggregate was added, the mixing continued for several minutes to insure a consistent distribution of ingredients.

The machined steel mold contained twenty-four 2 by 2 by 4 inch compartments. Normally 12 blocks were cast for each mixture. The compartments were filled about one-third full and then rodded 25 to 30 times. This process was repeated two more times to fill the mold. Additional mortar was spread over the top and worked down with a trowel. The excess mortar was removed leaving the mortar in the mold level with the top. The mold

was then covered with moistened burlap and allowed to stand for two days. The blocks were removed from the mold, and six blocks were stored in water, while six were stored in air. The blocks stored in water are defined as standard blocks, and the blocks stored in air are defined as air dried.

The absorption coefficient was determined both 14 and 28 days after the blocks were cast. The air dried blocks had only to be weighed and then tested as absorbers. The standard blocks were removed from the water tanks and blotted dry with paper towels to remove the surface moisture. They were then weighed and tested as absorbers. After the 14 day test, the water cured blocks were returned to the water tanks. The time required for these blocks to be out for the water was normally not over two hours.

The volume of all the blocks was considered to be constant. After determining the weight, the density was computed in gm/cm^3. Using a two-inch thickness, the absorber thickness in gm/cm^2 was computed for each block. The blocks were then used as absorbers and the counting rate was determined for 2 inch intervals of absorbers up to a total of ten inches. The corrected count versus absorber thickness was plotted on semi-log paper. The slope of the straight line obtained was the mass absorption coefficient, μ/ρ . Using the average density obtained from 6 blocks, the linear absorption coefficient was computed for both the air dried and standard blocks for each mixture.

At the start of each day, the source was removed from the area and a background count was taken. All counting data were corrected for this background. The background count was checked every three hours during the remainder of the day. After returning the source to the apparatus, several points on a plateau curve were taken to insure satisfactory

operation of the detector tube.

Since maximum counting rate for zero absorber was about 3,000 counts per minute, no correction was made for counter dead time.

The standard deviation for all counting data was maintained below 2 percent as this was the maximum predicted error for single scattered radiation.

The compressive strength of the mortar blocks was determined 28 days after casting. Three blocks from both the air dried and standard samples for each mixture were tested. All compressive tests were made along the four inch length of the blocks. The average of the three blocks was reported as the compressive strength. After being used as absorbers, the standard blocks were returned to the water tanks for several hours before they were tested for compressive strength. This permitted the blocks to regain any moisture they might have lost.

As a representative sample the data obtained for mixture E has been included in the Appendix.

Tests were conducted to determine if the orientation of the mortar blocks had any effect on the results. Two blocks each from five different mixtures were selected at random. The counting rate was determined for a two inch thickness of each block. The block was then rotated 90 degrees about the four inch axis, and the counting rate was determined a second time for a two inch thickness of the same block. Comparing the two counting rates for each block it was determined that, with two exceptions, the deviation between the counting rates was less than the standard deviation. The two exceptions were both air dried blocks from mixture H. The two counting rates for each of these blocks deviated from the average counting

rate for each block by 1.48 percent and 1.59 percent. The standard deviation for the same two blocks were 1.18 percent and 1.17 percent respectively.

Two blocks from each mixture were used jointly, each block providing two inches of absorber for a total of four inches of absorber, and the counting rate was determined. Each block was then used separately to provide four inches of absorber, and the counting rate was determined. Comparing the three counting rates obtained for each mixture, it was determined that the deviations were less than the standard deviations in all five mixtures.

These tests indicated that the absorption coefficients obtained for the mixtures were independent of the orientation of the blocks used as absorbers. It should be noted that while the deviations in counting rates for several of the blocks did not exceed the standard deviations, they did approach the standard deviations. The mixtures for which this occured are noted in the section on Results and Discussion as being porous.

VI. RESULTS AND DISCUSSION

The tabulated results for the 14 and 28 day absorption coefficient tests, as well as the 28 day compression tests, are given in Table 4. The absorption curves for the 28 day tests only are shown in Figure 4 to Figure 11. As an aid in evaluating the results, the densities, linear absorption coefficients, and the compressive strengths were plotted versus the percentage of slag content. These results are shown in Figure 12, 13 and 14, respectively.

The plot of density versus slag content, Figure 12, indicates not only the average density for five blocks, but also the spread of these densities. The standard mixture B, 17 percent slag, and air dried mixture C, 35 percent slag, show marked decreases in density. This density decrease causes a decrease in the linear absorption coefficient, as is obvious in Figure 13. The compressive strength for these two points also takes a definite drop as shown in Figure 14. This indicates that the samples in question were probably too porous. The only apparent explanation for this porosity is that there was a deviation in the mixing, or casting technique. The general trend shown in Figure 12 is for the density to increase to a maximum and then drop off. The compression strength decreases with increased slag as shown in Figure 14. This indicates the mixtures are becoming increasingly porous. This porosity was evident by the surface condition of the blocks as shown in the photograph in Figure 15. The results of the screen tests for the sand and slag are plotted in Figure 16 which clearly shows the slag to be more coarse.

Table 4. Composition and experimental results of the mixtures tested

Item	Units	Mixture A	B	C	D	E	F	G	H
Composition	Percent								
Cement	by	17.25	17.45	17.40	17.77	18.10	17.85	17.85	16.20
Water	weight	10.35	10.45	10.45	10.65	10.90	10.60	10.60	9.75
Sand		72.40	54.65	37.30	18.33	0	13.49	0	0
Slag		0	17.45	34.85	53.25	71.00	53.6	67.09	70.00
Fly ash		0	0	0	0	0	4.46	4.46	4.05
14 day test									
Standard									
Density	gm/cm^3	-	2.28	2.35	2.38	2.38	2.42	2.47	2.38
Mass absorption	cm^2/gm	-	.0566	.0566	.0563	.0558	.0563	.0555	.0563
Linear absorption	cm^{-1}	-	.129	.133	.135	.133	.136	.137	.134
Air dried									
Density	gm/cm^3	-	2.24	2.19	2.27	2.25	2.32	2.34	2.29
Mass absorption	cm^2/gm	-	.0572	.0575	.0568	.0560	.0573	.0569	.0563
Linear absorption	cm^{-1}	-	.128	.126	.129	.126	.133	.133	.129
28 day test									
Standard									
Density	gm/cm^3	2.32	2.28	2.35	2.38	2.36	2.41	2.48	2.37
Mass absorption	cm^2/gm	.0565	.0563	.0560	.0560	.0555	.0562	.0564	.0560
Linear absorption	cm^{-1}	.132	.128	.132	.133	.131	.136	.140	.133
Air dried									
Density	gm/cm^3	2.17	2.19	2.18	2.26	2.21	2.29	2.30	2.26
Mass absorption	cm^2/gm	.0587	.0576	.0566	.0563	.0558	.0550	.0564	.0560
Linear absorption	cm^{-1}	.127	.126	.123	.126	.123	.126	.130	.126
28 day compressive test									
Standard	lbs/in^2	3867	2433	2675	2617	2067	4383	3708	2583
Air dried	lbs/in^2	3600	3106	2725	3167	2375	4275	3200	3083

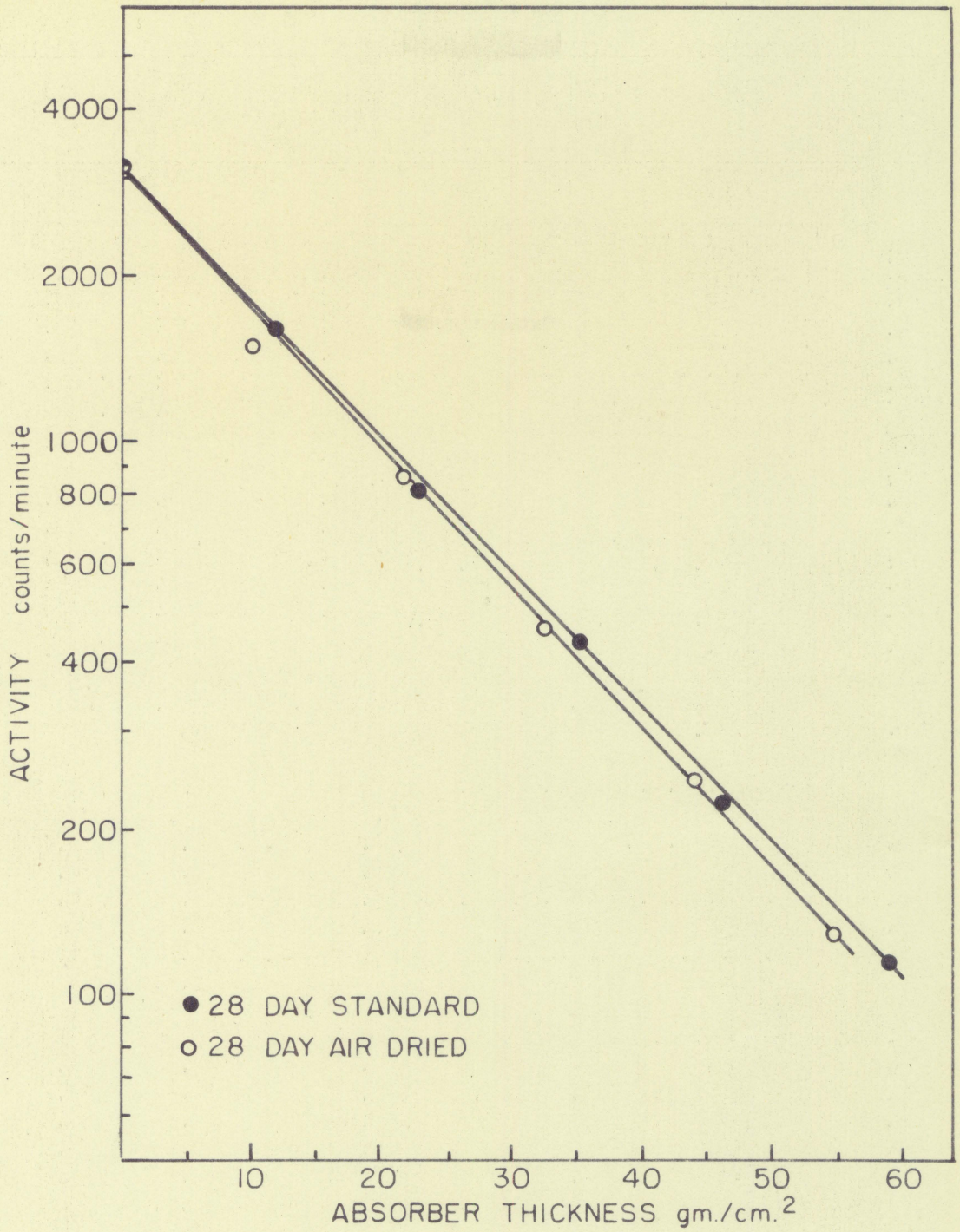

Figure 4. Mixture A absorption curve.

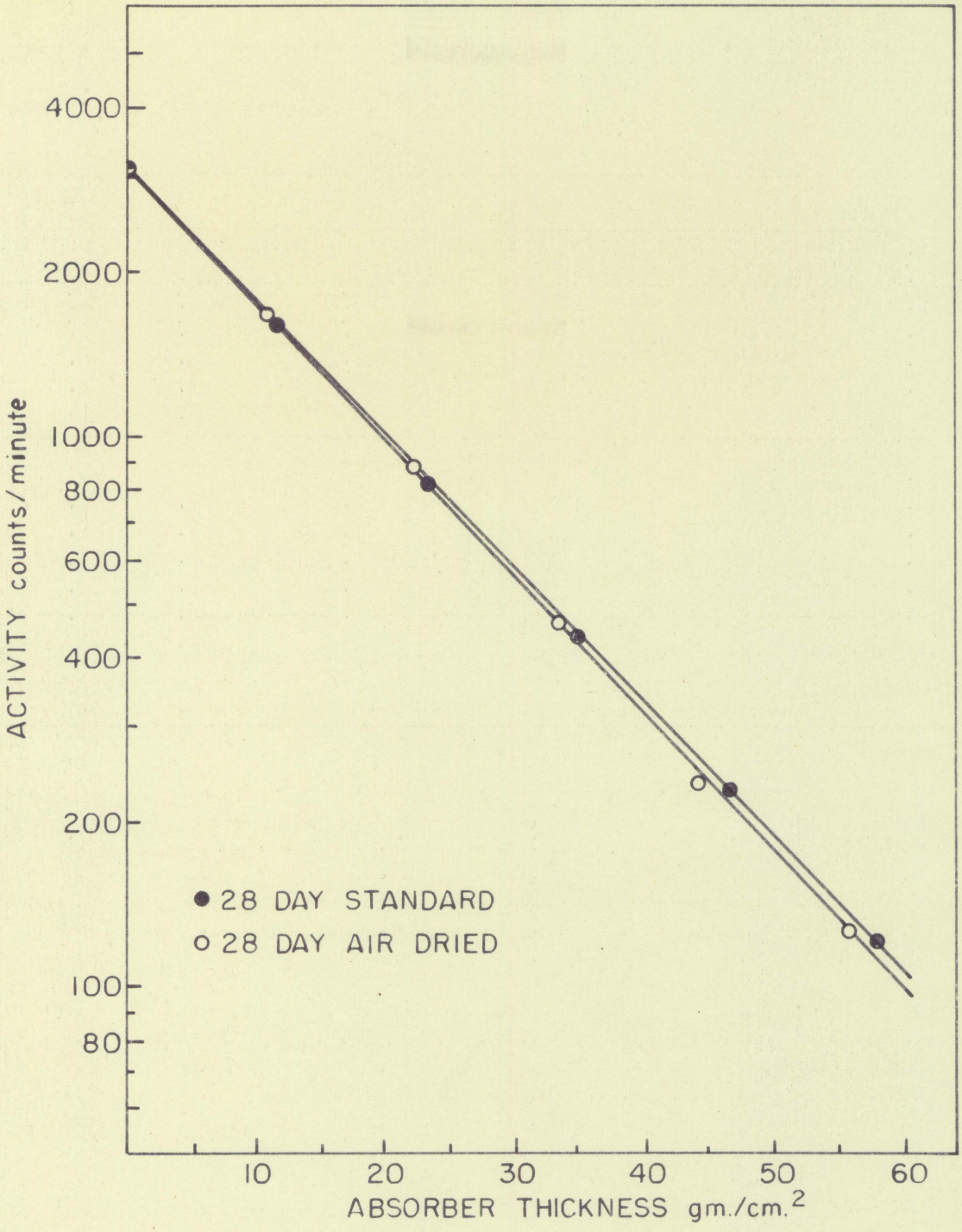

Figure 5. Mixture B absorption curve.

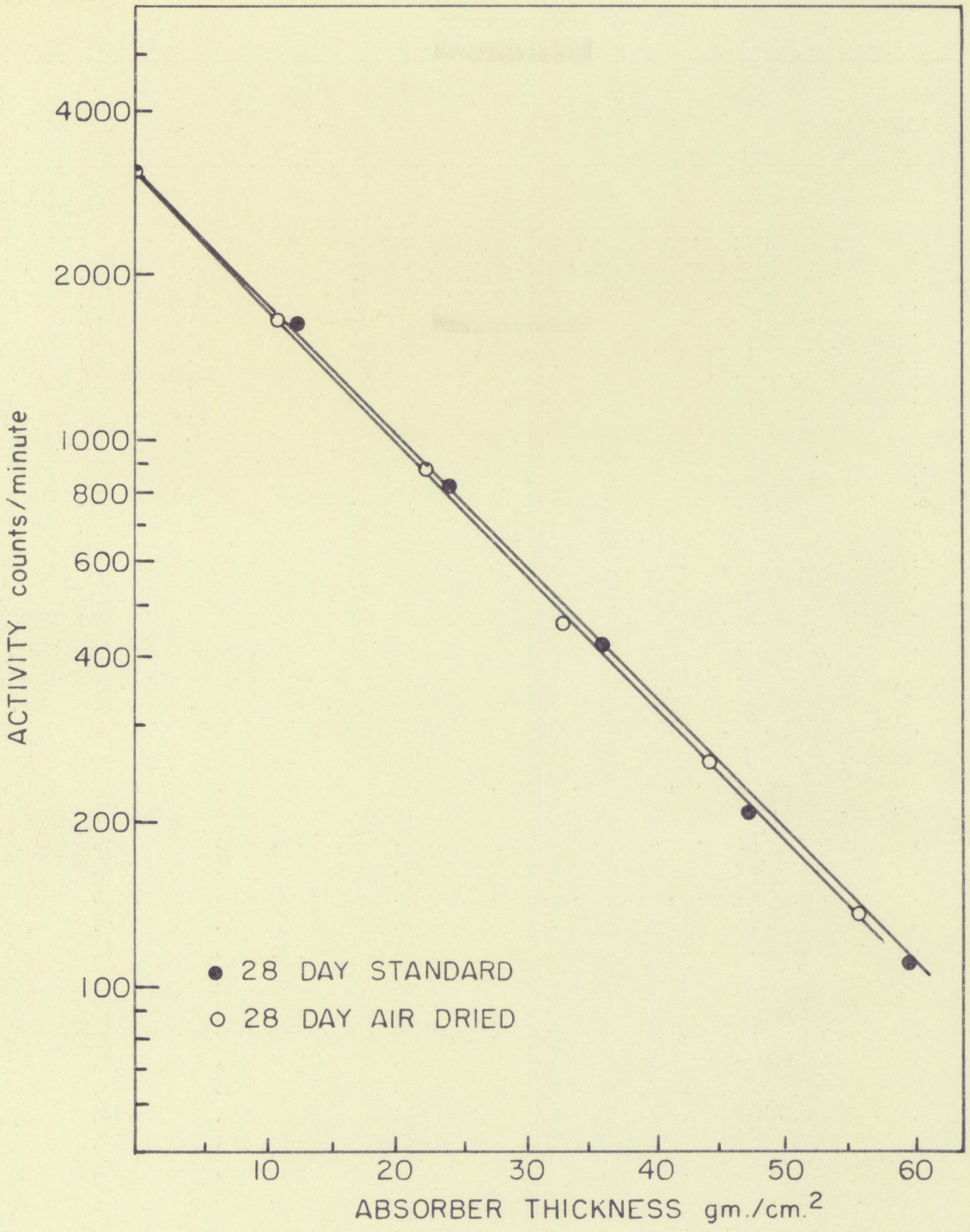

Figure 6. Mixture C absorption curve.

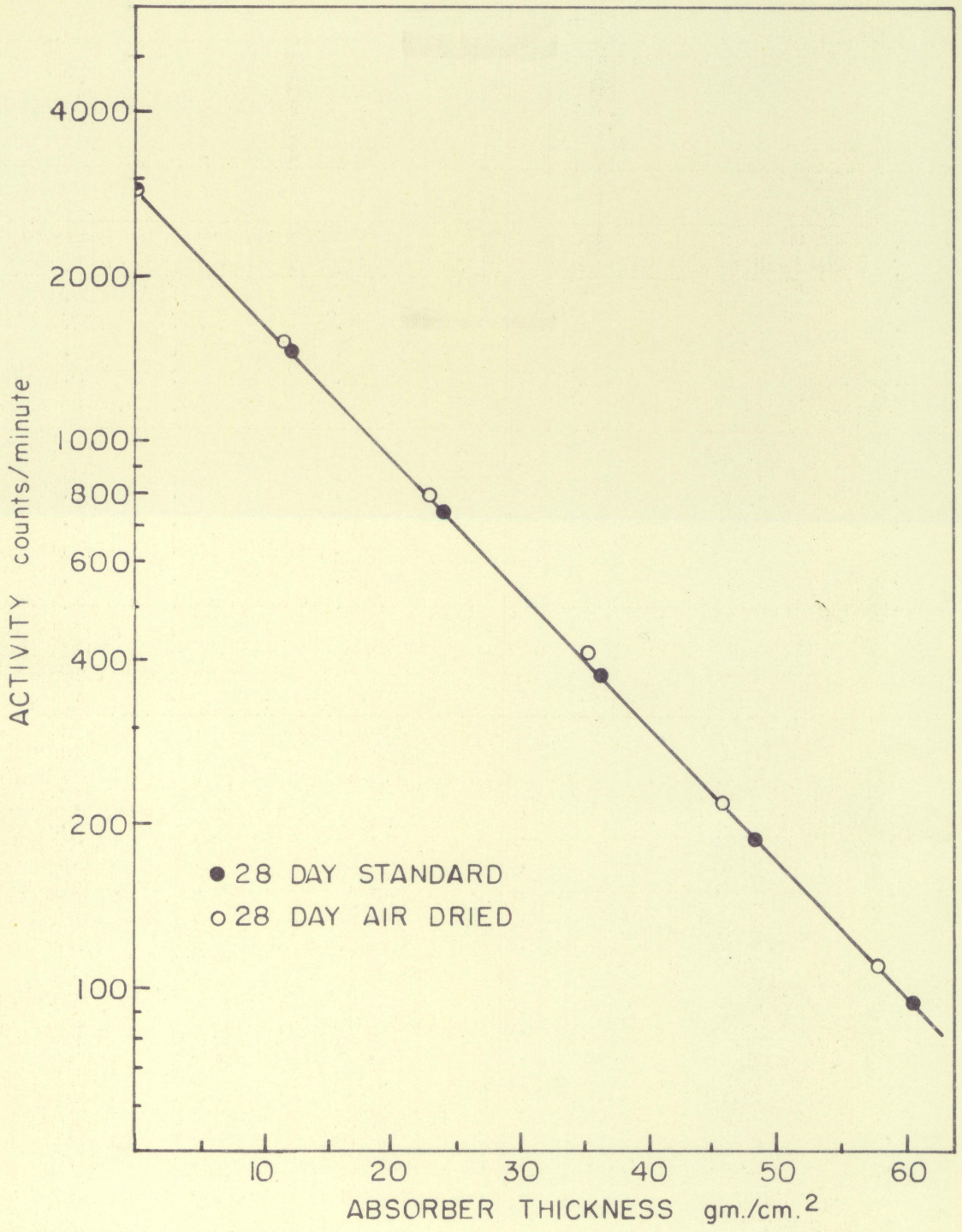

Figure 7. Mixture D absorption curve.

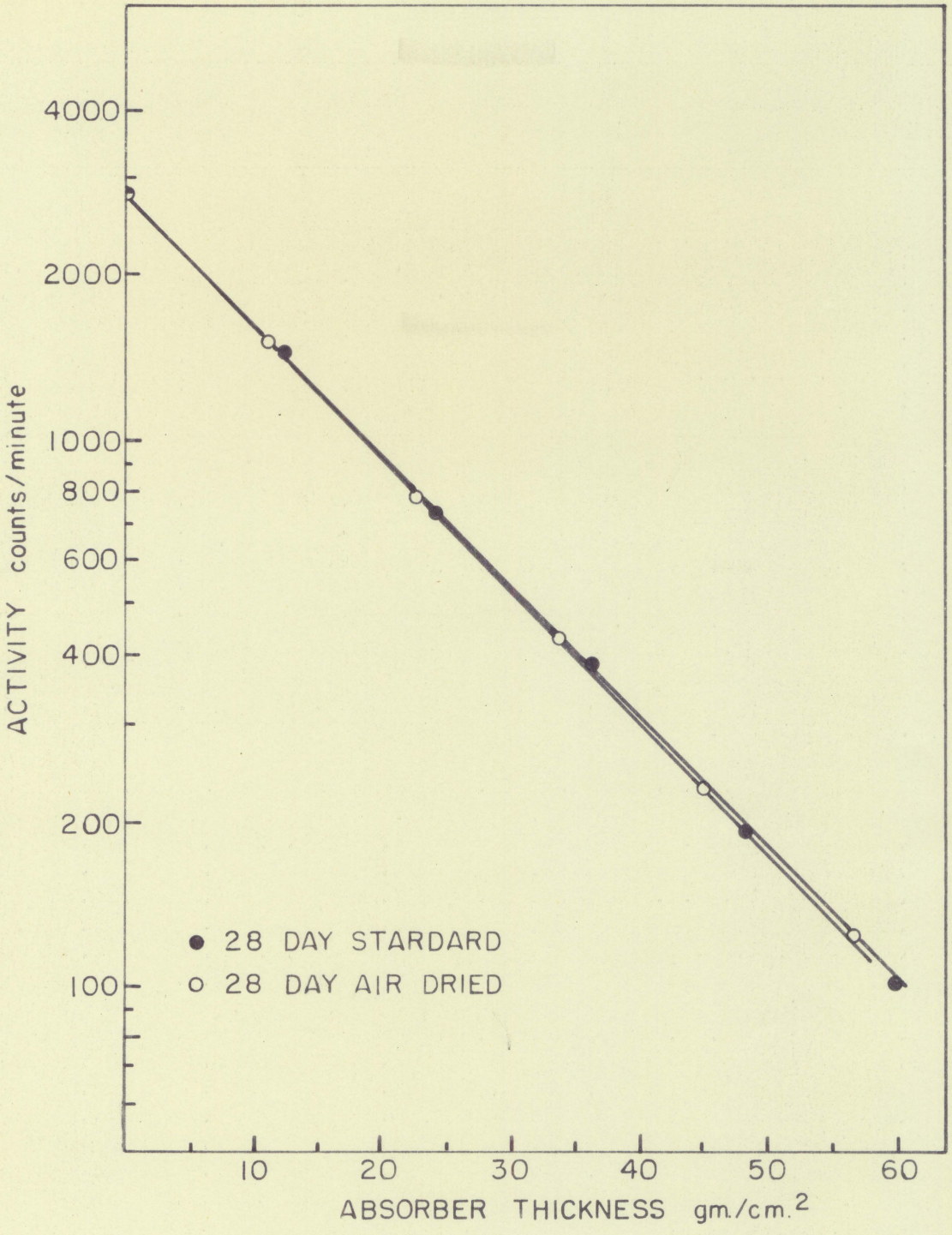

Figure 6. Mixture B absorption curve.

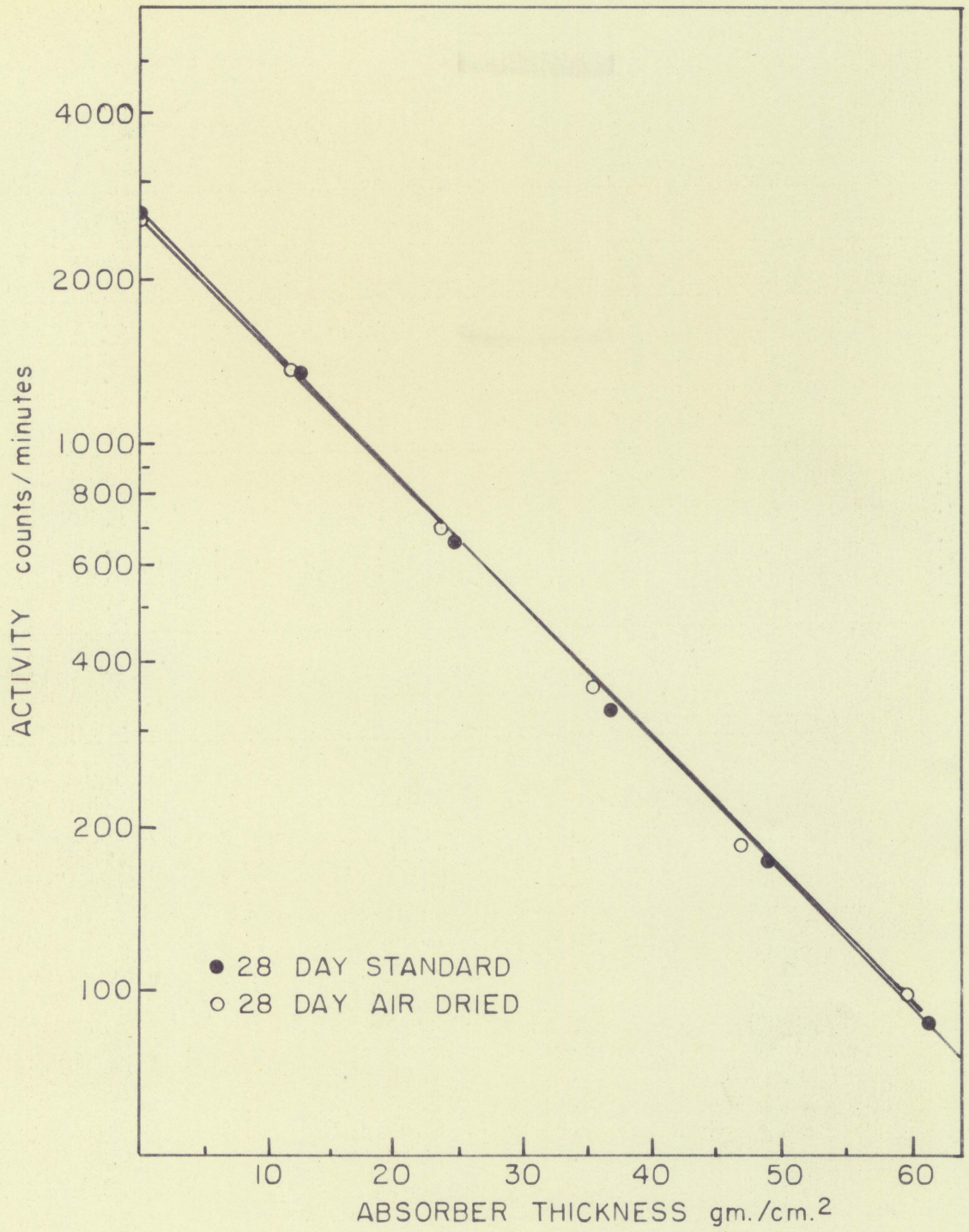

Figure 9. Mixture F absorption curve.

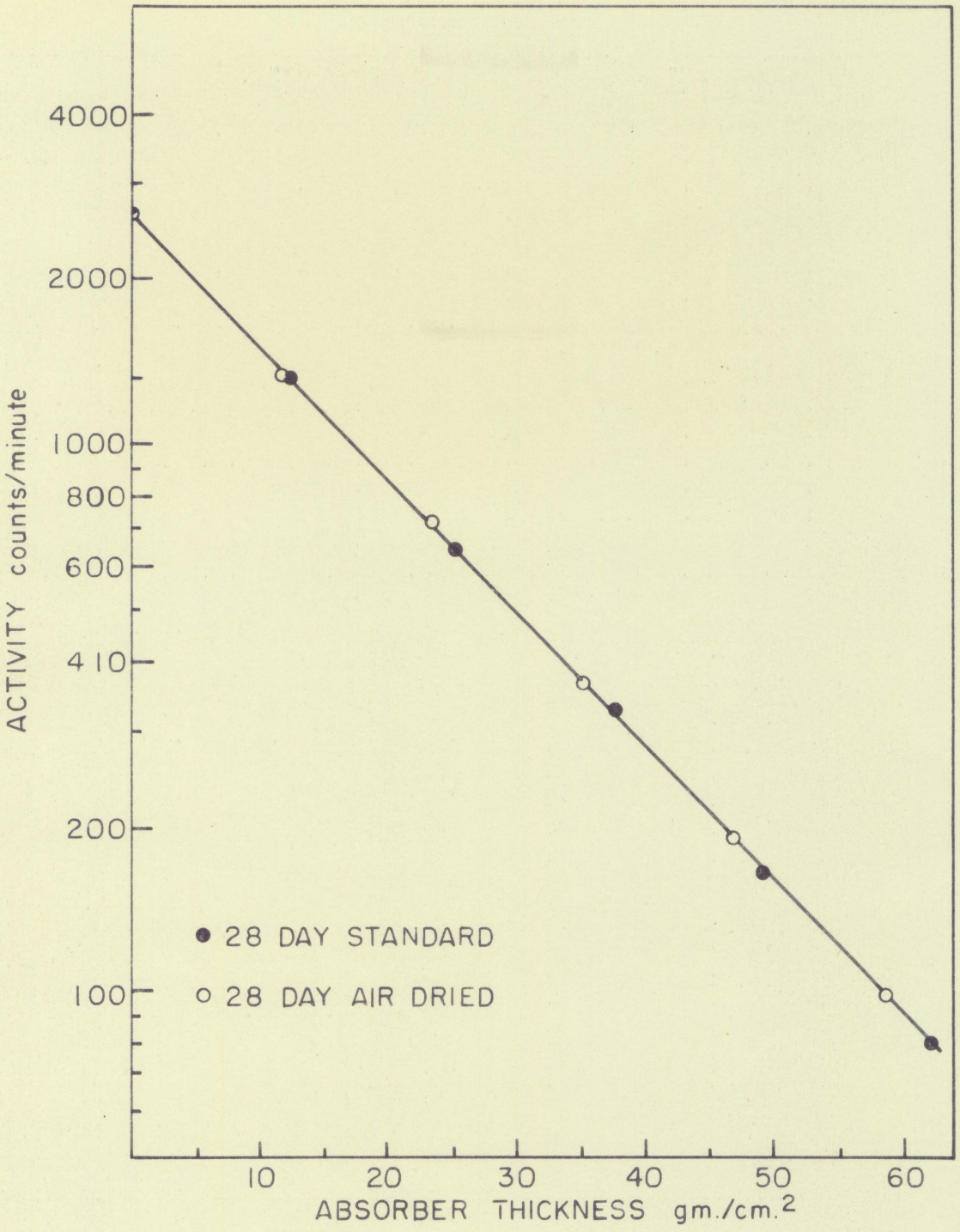

Figure 10. Mixture G absorption curve.

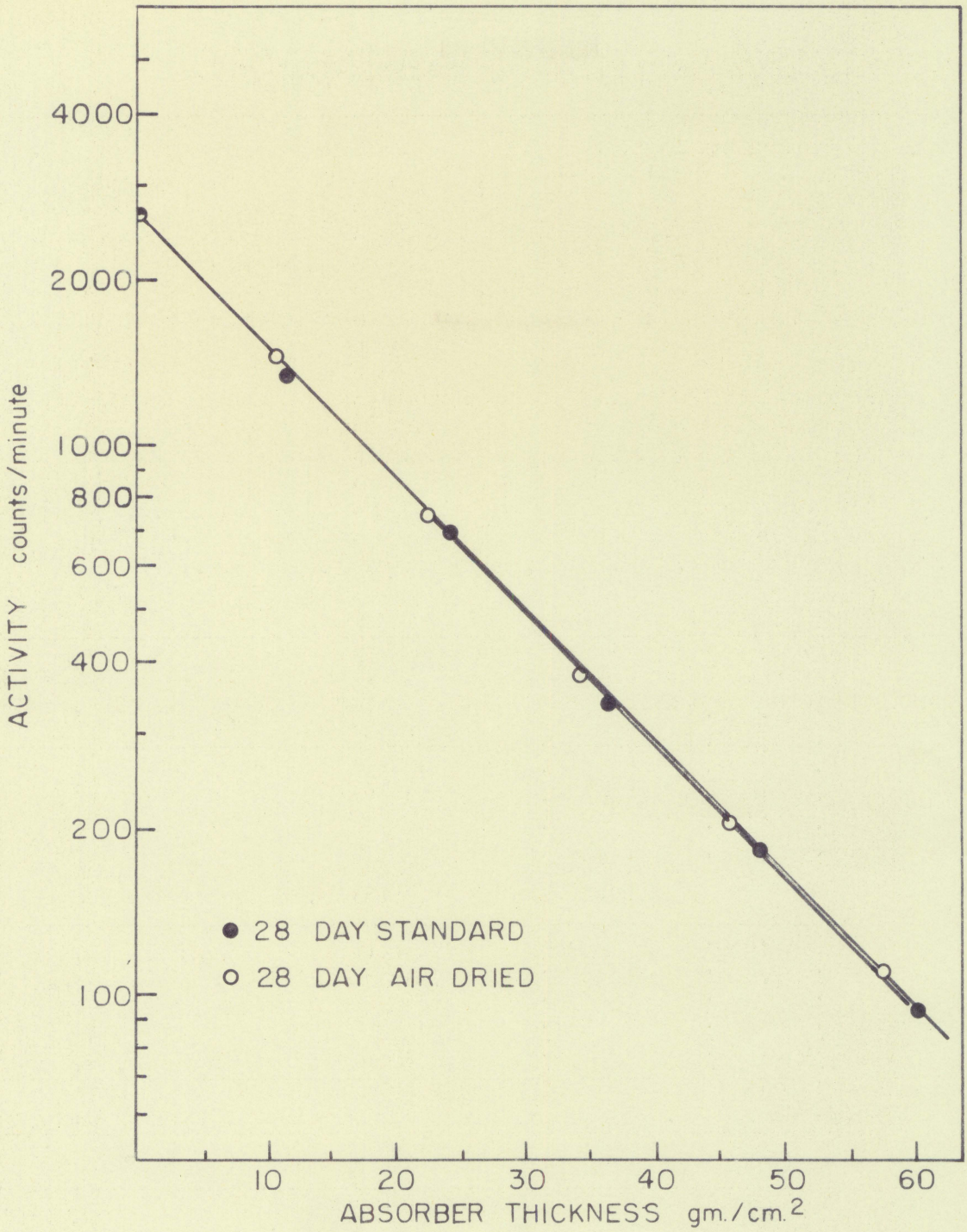

Figure 11. Mixture II absorption curve.

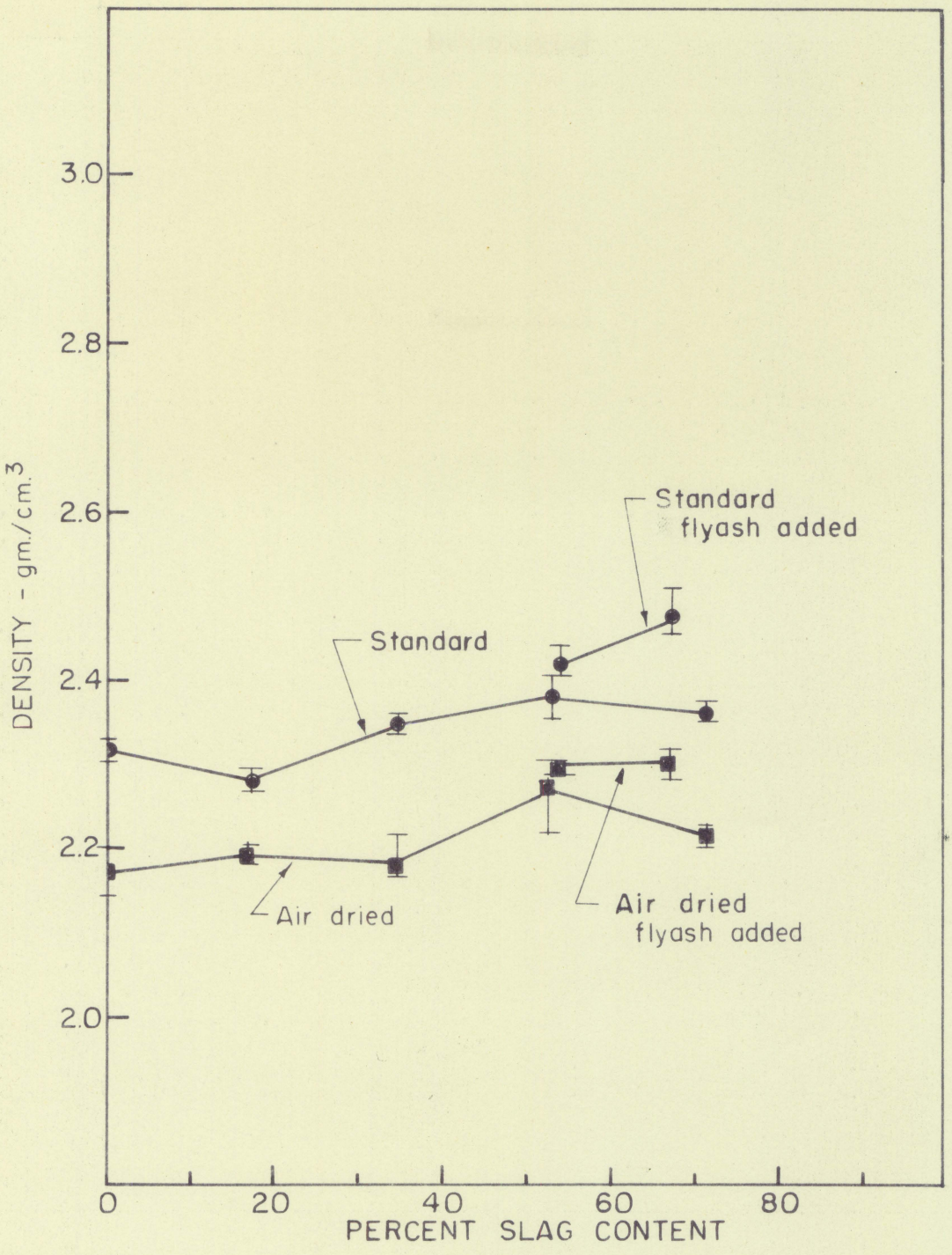

Figure 12. Variation of specimen density at 28 days with slag content.

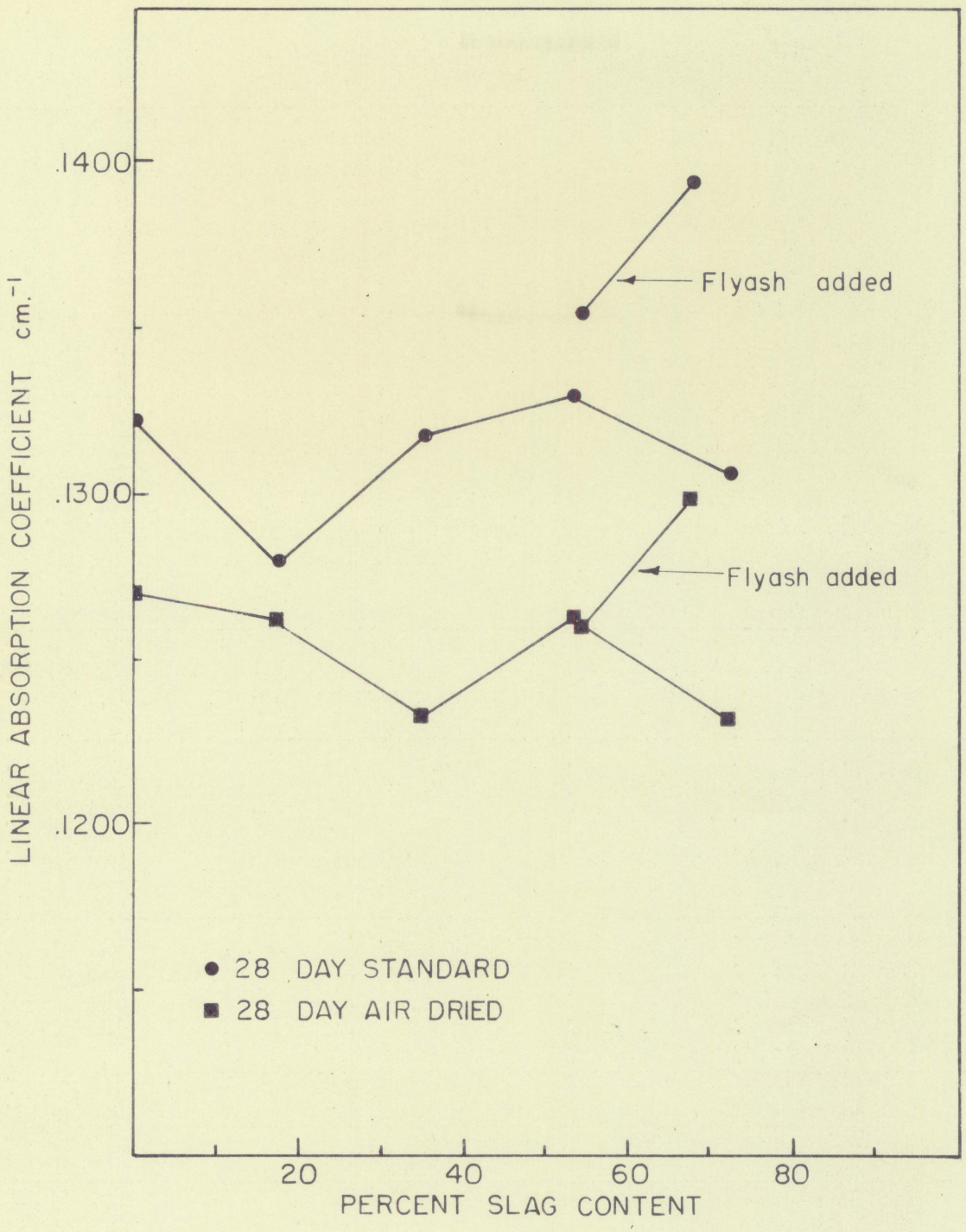

Figure 13. Variation of linear absorption coefficient with slag content.

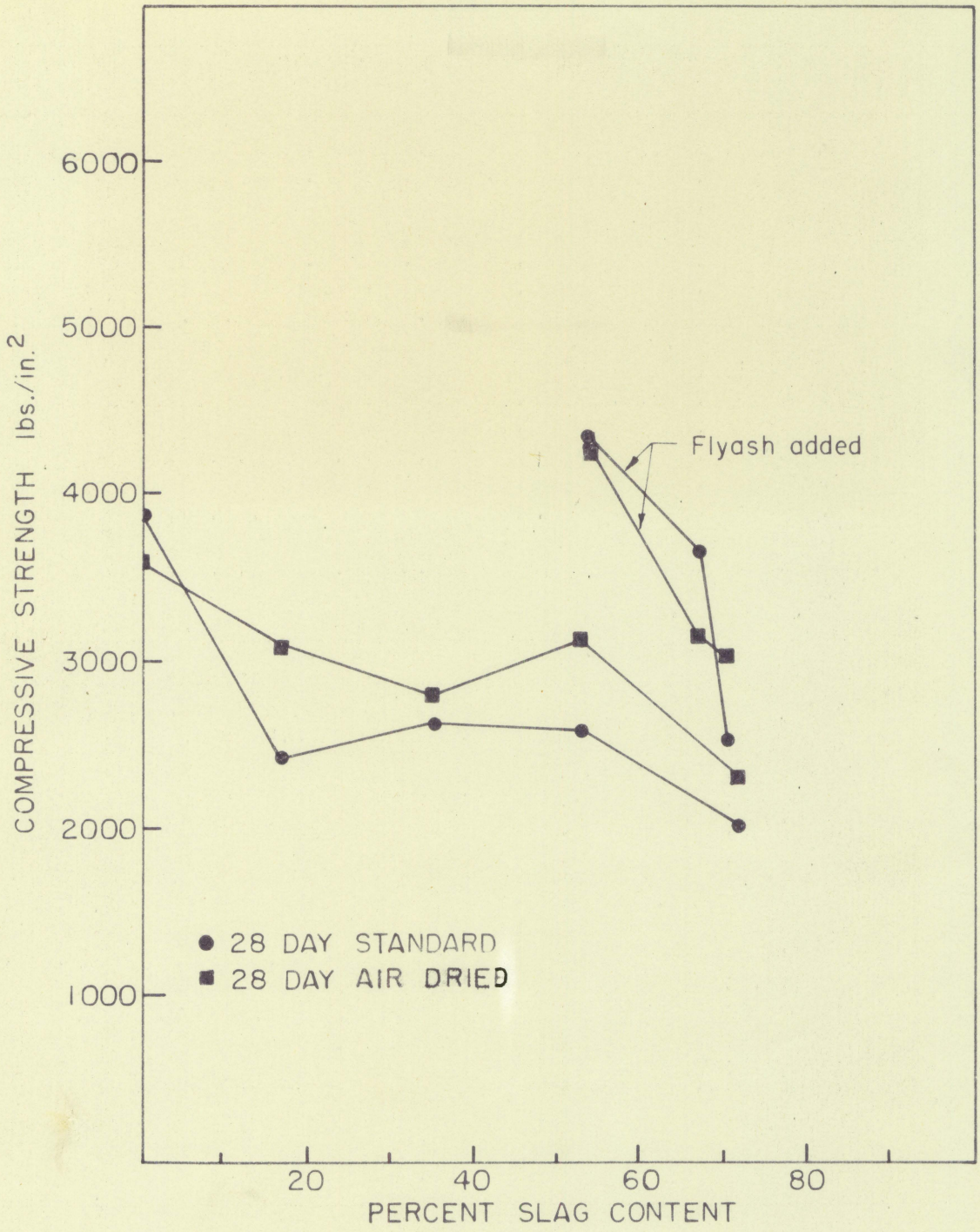

Figure 14. Variation in compressive strength with slag content.

Figure 15. Photograph showing surface condition of test blocks.

The net result of this test data is that, while the slag increases the density, it also increases the porosity and there is no gain in the linear absorption coefficient. In fact, the absorption coefficient decreases with increased slag.

The addition of fly ash with the slag eliminates the coarse effects of the slag in the aggregate. There is a substantial increase in density as shown in Figure 12. The compression strength drops when no sand is used as shown in Figure 14, but the absorption coefficient increases as shown in Figure 13. There is a maximum increase in the absorption coefficient of 5.5 percent for the standard blocks and a 2.4 percent increase for the air dried blocks.

Since the chemical analysis of the ingredients was not available no

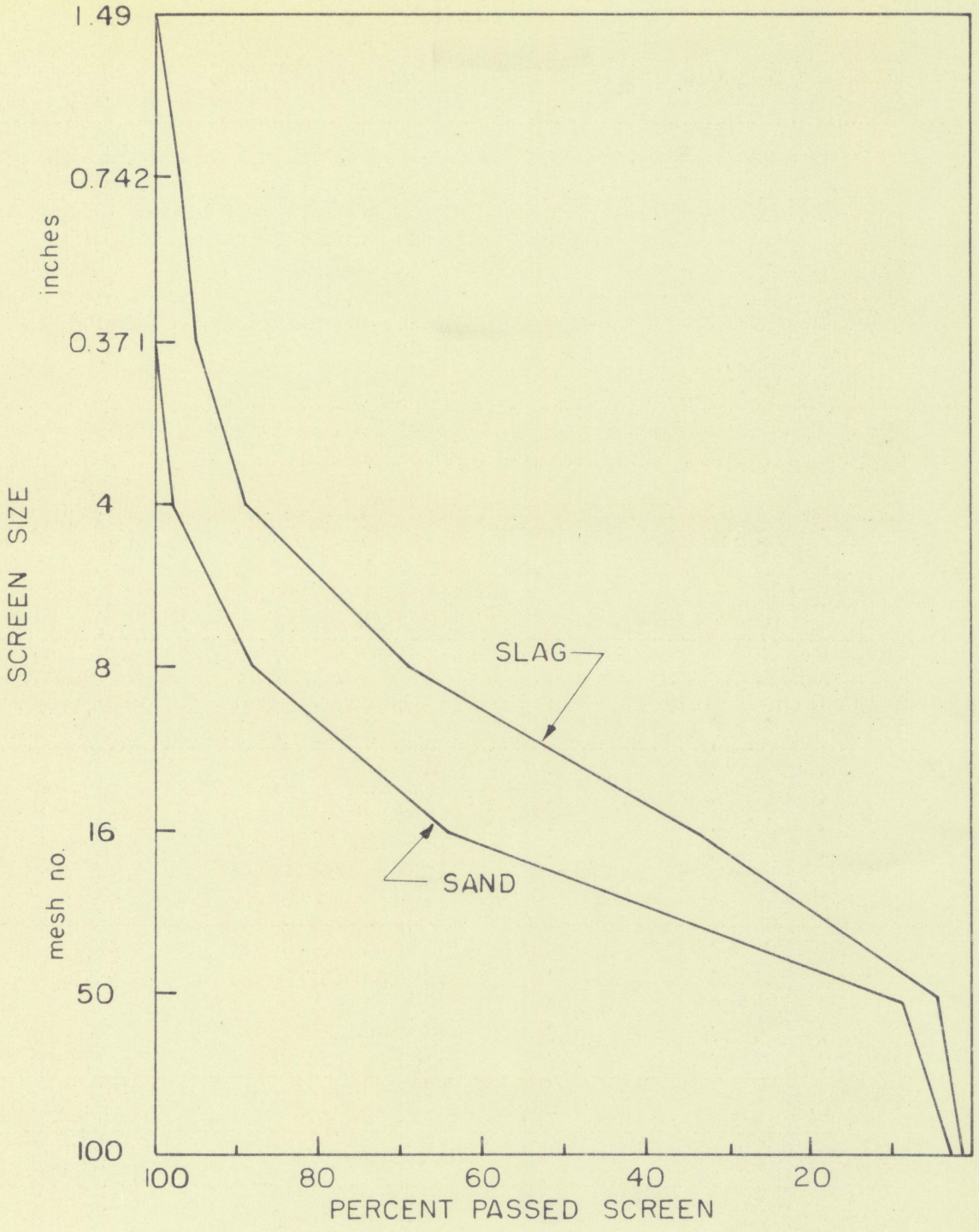

Figure 16. Particle size distribution of sand and slag.

exact comparison of theory and experiment could be made. In order to compare the trends indicated by the experimental tests with the theory, the absorption coefficients were computed for mixtures A to E. The compositions as reported in Table 1 were those used for this analysis. The absorption coefficients were computed for an incident photon energy of 1.25 Mev.

The linear absorption coefficients for all the elements that appear in Table 1 were computed using the formulas presented by Siri (10). The partial linear absorption coefficients for the elements were computed using the following equations:

Photoelectric effect,

$$\tau = 4.07\ \tau_{Pb}\ \frac{\rho_E Z^4}{A} \times 10^{-7}$$

Compton effect,

$$\sigma = 0.224\ \sigma_{Pb}\ \frac{\rho_E Z}{A}$$

Pair Production,

$$\varkappa = 2.725\ \varkappa_{Pb}\ \frac{\rho_E Z^2}{A} \times 10^{-3}\ .$$

The values used for lead were obtained from curves as $\tau_{Pb} = 0.14$, $\sigma_{Pb} = 0.51$ and $\varkappa_{Pb} = 0.002$. The total linear absorption coefficient is the sum of the partial coefficients, or $\mu = \tau + \sigma + \varkappa$. The mass absorption coefficient was obtained by dividing by the density of the element at 15° C. The computed mass absorption coefficients are shown in Table 5.

Table 5. Mass absorption coefficients

Element	μ/ρ cm^2/gm
H	.1140
O	.0577
Mg	.0572
Al	.0550
Si	.0573
Ca	.0574
Fe	.0533

As a check on these values, the values listed by Hungerford (5, pp. 718-719) for the elements, at energy values of 0.5, 1, 2, and 3 Mev. were plotted. The values determined from these curves at 1.25 Mev. agree with the above listed values.

The mass absorption coefficient for a mixture or compound was determined by the formula given by Fano (11, pp. 641-642), that is

$$\mu/\rho = \frac{\mu_1}{\rho_1} f_1 + \mu_2/\rho_2 \; f_2 + \ldots\ldots$$

where f_1, f_2, etc. are the fractional weight percentages of the element present. As an example, the mass absorption coefficient for SiO_2 was obtained, using the values listed in Table 5, as

$$\mu/\rho = 28/60\ (.0573) + 32/60\ (.0577) = 0.0576\ .$$

The values computed for all the compounds present in the mortar are listed in Table 6.

Table 6. Mass absorption coefficient of some compounds

Compound	μ/ρ cm^2/gm
H_2O	.0640
SiO_2	.0576
Fe_2O_3	.0546
Al_2O_3	.0563
CaO	.0575
MgO	.0574

The mass absorption coefficients for the cement and slag were obtained by the same method used to determine the values of the compound. The values are shown in Table 7.

It was necessary to determine the amount of the initial water that was retained in the mortar blocks. One standard block from each mixture was permitted to dry out for a minimum of one week after the 28 day tests. These blocks lost, on the average, 3 percent of their weight when dry. Their dry weight averaged 2 percent higher than the corresponding air cured blocks. Assuming that the standard dry blocks had retained 30 percent of the initial amount of water, it was determined that the

Table 7. Mass absorption coefficient of mortar ingredients

Material	μ/ρ cm^2/gm
Cement	.0573
Sand	.0576
Slag	.0565
H_2O	.0630

standard wet blocks contained 50 percent of the initial water, and the air cured blocks contained 15 percent of the initial water.

Using the above figures, the weight percentages listed in Table 4, for cement and aggregate, were adjusted for the water loss. The mass absorption coefficients for the standard and air cured condition were computed for mixtures A to E. These theoretical values are listed in Table 8 along with the experimentally determined values.

The theoretical values of the mass absorption coefficient indicate that there should be a 1.6 percent decrease in the mass absorption coefficient when slag is used as the aggregate. From Table 3, it was determined that the slag density is 9.8 percent greater than the density of the sand. To determine the density increase per block, the weight percentages for the standard blocks of mixtures A and E were converted to volume percentage. The volume percentage of sand in mixture A was 72.7 percent, while the volume percentage of slag in mixture E was 69.7 percent. The ratio of the volume percentage times the ratio of densities gives a

Table 8. Theoretical and experimental absorption coefficients

Mixture	μ/ρ cm^2/gm			
	Standard		Air dried	
	Theory	Experiment	Theory	Experiment
A	.0579	.0565	.0576	.0587
B	.0577	.0563	.0574	.0576
C	.0575	.0560	.0572	.0566
D	.0573	.0560	.0570	.0563
E	.0570	.0555	.0567	.0558

percentage weight increase of 5.0 percent. Since the blocks were the same volume, this is also the density increase.

The mass absorption coefficient decreases 1.6 percent while the density is increasing 5.0 percent. The linear absorption coefficient should therefore increase approximately 3.2 percent by replacing the sand with slag. The results show that this increase is not obtained. It is believed that the failure was caused by the porosity of the mixtures.

Since no information was available concerning the composition of the fly ash, a similar theoretical analysis could not be performed for mixtures F and G. The experimental results indicate that the use of fly ash and slag leads to a definite increase in the linear absorption coefficient.

VII. CONCLUSIONS

The results of the tests of the gamma ray shielding properties of mortars containing slag indicate that the following conclusions seem justified:

1. The use of slag as a fine aggregate may result in a porous mortar. The shielding properties of this mortar are reduced as a result of this porosity.
2. The use of fly ash in conjunction with slag as the fine aggregate in mortar shows an increase in the linear absorption coefficient of from 2.5 percent to 5 percent.
3. The use of water to keep the mortar saturated resulted in an increase of from 5 percent to 7 percent regardless of the aggregate used.
4. Additional research could be conducted to determine the ratio of sand, slag and fly ash which gives the optimum linear absorption coefficient.

VIII. LITERATURE CITED

1. Callaher, R. B. and Kitses, A. S. Summary report on Portland cement concretes for shielding. Oak Ridge National Laboratory 1414, Oak Ridge, Tenn. March, 1953.

2. Kaplan, Irving. Nuclear physics. Addison Wesley Publishing Co., Cambridge, Mass. 1956.

3. Davisson, C. M. and Evans, R. D. Gamma ray absorption coefficients. Review of Modern Physics 24:79-107. 1952.

4. Snyder, N. J. Cement and concretes. In U.S. Atomic Energy Commission Technical Information Service. The reactor handbook, vol. 3, chapt. 1.8. Tech. Info. Service, Oak Ridge, Tenn. March, 1955.

5. Hungerford, N. B. Shield materials. In U.S. Atomic Energy Commission Technical Information Service. The reactor handbook, vol. 1, chapt. 2.9. Tech. Info. Service, Oak Ridge, Tenn. March, 1955.

6. Davis, N. S. How to choose and place mixes for high density concrete reactor shields. Nucleonics 13, no. 6: 60-65. June, 1955.

7. Lane, J. A. How to design reactor shields for lowest cost. Nucleonics 13, no. 6: 65. June, 1955.

8. Davisson, C. M. and Evans, R. D. Measurements of gamma ray absorption coefficients. Physical Review 81: 404-411. 1951.

9. Heitler, W. The quantum theory of radiation. 2nd ed. Oxford University Press, Oxford, England. 1944.

10. Siri, William, ed. Handbook of radioactive and tracer methodology. U.S.A.F. Material Command, Wright Patterson A.F.B., Dayton, Ohio. 1948.

11. Fano, U. Gamma ray attenuation. In U.S. Atomic Energy Commission Technical Information Service. The reactor handbook, vol. 1, chapt. 2.3. Tech. Info. Service, Oak Ridge, Tenn. March, 1955.

IX. ACKNOWLEDGMENTS

This study was conducted as a part of the graduate program in Engineering with a minor in Nuclear Science. Participation in this course of study was sponsored by the United States Navy Post Graduate School, Monterey, California.

The author wishes to express appreciation to Dr. Glenn Murphy for his helpful suggestions, criticism and encouragement.

Thanks are extended to the Chicago Fly Ash Company for providing the slag and fly ash used in this study.

X. APPENDIX

APPENDIX

Data for Mixture E

Table 9. Composition

Date	Material	Weight lbs.	Percent weight
3/6/57	Cement	4.0	18.10
	Water	2.4	10.90
	Slag	15.65	71.00
	Sand	0	0

Table 10. 14 day test data. Date: 3/20/57

Item	Wt. lbs.	Density gm/cm^2	Thickness cm^2/gm	Count	Time min.	Net	Percent deviation
Background				452	30	16± 1	
Standard							
1	0	0	0	15,101	5	3005±24	0.8
2	1.38	2.38	12.12	9,268	6	1530±16	1.0
3	1.38	2.38	24.24	8,094	10	794± 9	1.1
4	1.38	2.38	36.36	6,375	15	410± 5	1.2
5	1.37	2.37	48.41	4,374	20	204± 3	1.5
6	1.37	2.37	60.46	2,966	25	104± 2	1.9
	Av.	2.38					
Air dried							
1	0	0	0	14,893	5	2964±24	0.8
2	1.31	2.27	11.52	9,799	6	1618±16	1.0
3	1.30	2.25	22.96	8,404	10	825± 9	1.0
4	1.29	2.23	34.28	6,814	15	438± 6	1.4
5	1.31	2.27	45.80	5,063	20	238± 4	1.7
6	1.29	2.23	57.12	3,370	25	119± 2	1.7
	Av.	2.25					

Table 11. 28 day test data. Date: 4/3/57

Item	Wt. lbs.	Density gm/cm³	Thickness cm²/gm	Count	Time min.	Net	Percent deviation
Background				425	30	14± 1	
Standard							
1	0	0	0	14,134	5	2813±24	0.9
2	1.37	2.37	12.05	7,172	5	1420±17	1.2
3	1.37	2.37	24.10	7,506	10	737± 9	1.2
4	1.36	2.35	36.05	5,985	15	385± 5	1.3
5	1.36	2.35	48.00	4,058	20	189± 5	1.6
6	1.36	2.35	59.95	2,851	25	100± 2	2.0
	Av.	2.36					
Air dried							
1	0	0	0	14,037	5	2793±24	0.9
2	1.28	2.22	11.25	7,556	5	1497±17	1.1
3	1.28	2.22	22.50	7,998	10	786± 9	1.1
4	1.29	2.23	33.83	6,645	15	429± 5	1.2
5	1.27	2.20	45.00	4,837	20	228± 4	1.8
6	1.27	2.20	56.17	3,370	25	121± 2	1.7
	Av.	2.21					

Table 12. Compressive test data. Date: 4/3/57

Standard			Air dried		
Item	Force lbs.	Stress lbs/in²	Item	Force lbs.	Stress lbs/in²
1	8300	2075	1	10,500	2625
2	8000	2000	2	9,200	2300
3	8500	2125	2	8,800	2200
		Av. 2067			Av. 2375